6.

Development of Building Damage Functions for Earthquake Loss Estimation

Charles A. Kircher, M.EERI, Aladdin A. Nassar, M.EERI, Onder Kustu, M.EERI, and William T. Holmes, M.EERI

This paper describes building damage functions that were developed for the FEMA/NIBS earthquake loss estimation methodology (Whitman et al., 1997). These functions estimate the probability of discrete states of structural and nonstructural building damage that are used as inputs to the estimation of building losses, including economic loss, casualties and loss of function (Kircher et al., 1997). These functions are of a new form and represent a significant step forward in the prediction of earthquake impacts. Unlike previous building damage models that are based on Modified Mercalli Intensity, the new functions use quantitative measures of ground shaking (and ground failure) and analyze model building types in a similar manner to the engineering analysis of a single structure.

INTRODUCTION

This paper describes methods for estimating the probability of discrete states of structural and nonstructural damage to buildings that were developed for the FEMA/NIBS earthquake loss estimation methodology. The FEMA/NIBS methodology has many components, or modules, as described in the paper by Whitman et al. (1997) in this issue. Components specific to the estimation of building losses are described in a companion paper by Kircher et al. (1997) in this issue. At the heart of loss estimation are the probabilities of structural and nonstructural damage calculated using building damage functions.

BUILDING DAMAGE FUNCTIONS

Two sets of functions, or curves, are used in the FEMA/NIBS methodology to estimate damage to buildings resulting from ground shaking: (1) capacity curves and (2) fragility curves. Capacity curves estimate peak response of buildings for a given level of spectral demand. These curves are analogous to "pushover" curves of individual buildings and are based on engineering parameters (e.g., yield and ultimate strength) of the structural system that characterize the nonlinear behavior of different model building types.

(CAK) Kircher & Associates, Mountain View, CA 94041
(AAN) GeoRisk, Mountain View, CA 94043
(OK) OAK Engineering, Belmont, CA 94002
(WTH) Rutherford & Chekene, San Francisco, CA 94107

The fragility curves predict the probability of reaching or exceeding specific damage states for a given level of peak earthquake response. The probability of being in a particular state of damage, the input used to predict building-related losses, is calculated as the difference between fragility curves.

Specific details are provided in the following sections on: (1) building classification by model building type and occupancy, (2) building design and performance levels, (3) structural and nonstructural systems and contents, and (4) building damage states.

BUILDING CLASSIFICATION

Buildings are classified both in terms of their use, or occupancy class, and in terms of their structural system, or model building type. Damage is predicted based on model building type, since the structural system is considered the key factor in assessing overall building performance, loss of function and casualties. Occupancy class is important in determining economic loss, since building value is primarily a function of building use (e.g., hospitals are more valuable than most commercial buildings, primarily because of their expensive nonstructural systems and contents, not because of their structural systems).

Twenty-eight occupancy classes are defined to distinguish among residential, commercial, industrial or other buildings, and 36 model building types are used to classify buildings within the overall categories of wood, steel, concrete, masonry or mobile homes. Building inventory data relate model building type and occupancy class on the basis of floor area, as illustrated in Figure 1, so that for a given geographical area the distribution of the total floor area of model building types is known for each occupancy class. For presentation purposes, Figure 1 shows only the four overall categories of occupancy and the five overall categories of construction, whereas FEMA/NIBS methodology calculations are based on all 28 occupancy classes and 36 model building types.
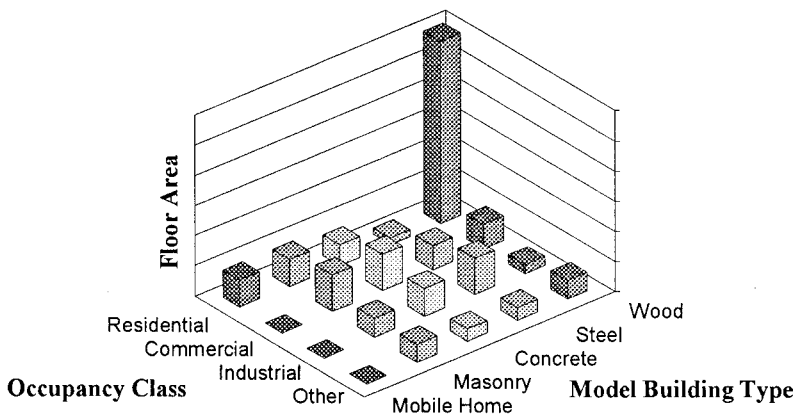

Figure 1. Example inventory relationship of model building type and occupancy class

Model building types are derived from the classification system of the *NEHRP Handbook for the Seismic Evaluation of Existing Buildings* (FEMA, 1992), expanded to include mobile homes, and considering building height. Table 1 describes model building types and their heights. Typical building heights are used in the determination of capacity curve properties.

Table 1. Model building types of the FEMA/NIBS methodology

No.	Label	Description	Height			
			Range		Typical	
			Name	Stories	Stories	Feet
1	W1	Wood, Light Frame (≤ 5,000 sq. ft.)		All	1	14
2	W2	Wood, Greater than 5,000 sq. ft.		All	2	24
3	S1L	Steel Moment Frame	Low-Rise	1-3	2	24
4	S1M		Mid-Rise	4-7	5	60
5	S1H		High-Rise	8+	13	156
6	S2L	Steel Braced Frame	Low-Rise	1-3	2	24
7	S2M		Mid-Rise	4-7	5	60
8	S2H		High-Rise	8+	13	156
9	S3	Steel Light Frame		All	1	15
10	S4L	Steel Frame with Cast-in-Place	Low-Rise	1-3	2	24
11	S4M	Concrete Shear Walls	Mid-Rise	4-7	5	60
12	S4H		High-Rise	8+	13	156
13	S5L	Steel Frame with Unreinforced	Low-Rise	1-3	2	24
14	S5M	Masonry Infill Walls	Mid-Rise	4-7	5	60
15	S5H		High-Rise	8+	13	156
16	C1L	Concrete Moment Frame	Low-Rise	1-3	2	20
17	C1M		Mid-Rise	4-7	5	50
18	C1H		High-Rise	8+	12	120
19	C2L	Concrete Shear Walls	Low-Rise	1-3	2	20
20	C2M		Mid-Rise	4-7	5	50
21	C2H		High-Rise	8+	12	120
22	C3L	Concrete Frame with Unreinforced	Low-Rise	1-3	2	20
23	C3M	Masonry Infill Walls	Mid-Rise	4-7	5	50
24	C3H		High-Rise	8+	12	120
25	PC1	Precast Concrete Tilt-Up Walls		All	1	15
26	PC2L	Precast Concrete Frames with	Low-Rise	1-3	2	20
27	PC2M	Concrete Shear Walls	Mid-Rise	4-7	5	50
28	PC2H		High-Rise	8+	12	120
29	RM1L	Reinforced Masonry Bearing Wall s	Low-Rise	1-3	2	20
30	RM1M	with Wood or Metal Deck Diaphragms	Mid-Rise	4+	5	50
31	RM2L	Reinforced Masonry Bearing Wall s	Low-Rise	1-3	2	20
32	RM2M	with Precast Concrete Diaphragms	Mid-Rise	4-7	5	50
33	RM2H		High-Rise	8+	12	120
34	URML	Unreinforced Masonry Bearing Walls	Low-Rise	1-2	1	15
35	URMM		Mid-Rise	3+	3	39
36	MH	Mobile Homes		All	1	12

BUILDING DESIGN AND PERFORMANCE LEVELS

The building damage functions distinguish among buildings that are designed to different seismic standards, or are otherwise expected to perform differently during an earthquake. These differences in expected building performance are determined on the basis of seismic zone location, design vintage and use (i.e., special seismic design of essential facilities).

The 1994 *Uniform Building Code* (ICBO, 1994) is used to establish differences in seismic design levels, since the 1994 *UBC* or earlier editions of this model code likely governed the

design, if the building was designed for earthquake loads. For the purpose of loss estimation, buildings designed in accordance with the 1994 *NEHRP Provisions* (FEMA, 1995) are assumed to have similar damage functions to buildings designed to meet the 1994 *UBC*. Damage functions are provided for three "Code" seismic design levels, labeled as High-Code, Moderate-Code and Low-Code, and an additional design level for Pre-Code buildings. The Pre-Code design level includes buildings built before seismic codes were required for building design (e.g., buildings built before 1940 in California and other areas of high seismicity).

High-Code, Moderate-Code and Low-Code seismic design levels are based on 1994 *UBC* lateral force design requirements of Seismic Zones 4, 2B and 1, respectively. Damage functions for these design levels are directly applicable to modern code buildings of 1973 or later design vintage. Pre-1973 buildings and buildings of other *UBC* seismic zones are associated with Moderate-Code, Low-Code or Pre-Code design levels, based either on the expertise of the user or on default relationships provided with the FEMA/NIBS methodology. For example, Moderate-Code (rather than High-Code) damage functions are used to estimate damage to *UBC* Seismic Zone 4 buildings built before 1973 (but after 1940).

The FEMA/NIBS methodology also includes "Special," above-Code, building damage functions for those essential facilities (e.g., post-1973 California hospitals) that are known to be of superior design and construction. Building damage functions for Special buildings are based on the same theory as that of Code buildings, except that the parameters of the capacity and fragility curves reflect greater seismic capacity and reliability of these buildings. While essential facilities are important, they typically represent only a very small fraction of buildings. This paper focuses on Code (and Pre-Code) building damage functions.

STRUCTURAL AND NONSTRUCTURAL SYSTEMS AND CONTENTS

Buildings are composed of both structural (load carrying) and nonstructural systems (e.g., architectural and mechanical components). While damage to the structural system is the most important measure of building damage affecting casualties and catastrophic loss of function (due to unsafe conditions), damage to nonstructural systems and contents tends to dominate economic loss. Typically, the structural system represents about 25% of the building's worth.

To better estimate different types of loss, building damage functions separately predict damage to: (1) the structural system, (2) drift-sensitive nonstructural components, such as partition walls that are primarily affected by building displacement, and (3) acceleration-sensitive nonstructural components, such as suspended ceilings, that are primarily affected by building shaking. Building contents are also considered to be acceleration sensitive. Distinguishing between drift- and acceleration-sensitive nonstructural components and contents permits more realistic estimates of damage considering building response.
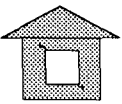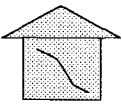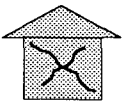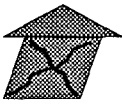
BUILDING DAMAGE STATES

Damage states are defined separately for structural and nonstructural systems of a building. Damage is described by one of four discrete damage states: Slight, Moderate, Extensive or Complete. Of course, actual building damage varies as a continuous function of earthquake demand. Ranges of damage are used to describe building damage, since it is not practical to have a continuous scale, and damage states provide the user with an understanding

of the building's physical condition. Loss functions relate the physical condition of the building to various loss parameters (i.e., direct economic loss, casualties, loss of function). For example, direct economic loss due to Moderate damage corresponds to 10% replacement value of structural and nonstructural components, on the average.

The four damage states of the FEMA/NIBS methodology are similar to the damage states defined in *Expected Seismic Performance of Buildings* (EERI, 1994), except that damage descriptions vary for each model building type based on the type of structural system and material. Table 2 provides structural damage states for W1 buildings (light frame wood) typical of the conventional construction used for single-family homes.

Table 2. Example damage states - light-frame wood buildings (W1)

Damage State		Description
	Slight	Small plaster cracks at corners of door and window openings and wall-ceiling intersections; small cracks in masonry chimneys and masonry veneers. Small cracks are assumed to be visible with a maximum width of less than 1/8 inch (cracks wider than 1/8 inch are referred to as "large" cracks).
	Moderate	Large plaster or gypsum-board cracks at corners of door and window openings; small diagonal cracks across shear wall panels exhibited by small cracks in stucco and gypsum wall panels; large cracks in brick chimneys; toppling of tall masonry chimneys.
	Extensive	Large diagonal cracks across shear wall panels or large cracks at plywood joints; permanent lateral movement of floors and roof; toppling of most brick chimneys; cracks in foundations; splitting of wood sill plates and/or slippage of structure over foundations.
	Complete	Structure may have large permanent lateral displacement or be in imminent danger of collapse due to cripple wall failure or failure of the lateral load resisting system; some structures may slip and fall off the foundation; large foundation cracks. Five percent of the total area of buildings with Complete damage is expected to be collapsed.

BUILDING CAPACITY CURVES

A building capacity curve is a plot of a building's lateral load resistance as a function of a characteristic lateral displacement (i.e., a force-deflection plot). It is derived from a plot of static-equivalent base shear versus building displacement at the roof, known commonly as a pushover curve. In order to facilitate direct comparison with spectral demand, base shear is converted to spectral acceleration and the roof displacement is converted to spectral displacement using modal properties that represent pushover response. Pushover curves and related-capacity curves, are derived from concepts similar to those of the *NEHRP Guidelines for the Seismic Rehabilitation of Buildings* (FEMA, 1997), and in *Seismic Evaluation and Retrofit of Concrete Buildings* (SSC, 1996), known as ATC-40.

Building capacity curves are constructed for each model building type and represent different levels of lateral force design and building performance. Each curve is defined by two control points: (1) the "yield" capacity, and (2) the "ultimate" capacity. The yield capacity represents the lateral strength of the building and accounts for design strength, redundancies

in design, conservatism in code requirements and expected (rather than nominal) strength of materials. Design strengths of model building types are based on the requirements of current model seismic code provisions (e.g., 1994 *UBC* or *NEHRP Provisions*) or on an estimate of lateral strength for buildings not designed for earthquake loads. Certain buildings designed for wind, such as taller buildings located in zones of low or moderate seismicity, may have a lateral design strength considerably greater than those based on seismic code provisions.

The ultimate capacity represents the maximum strength of the building when the global structural system has reached a full mechanism. Typically, a building is assumed capable of deforming beyond its ultimate point without loss of stability, but its structural system provides no additional resistance to lateral earthquake force. Up to yield, the building capacity curve is assumed to be linear with stiffness based on an estimate of the expected period of the building. From yield to the ultimate point, the capacity curve transitions in slope from an essentially elastic state to a fully plastic state. The capacity curve is assumed to remain plastic past the ultimate point. An example building capacity curve is shown in Figure 2.
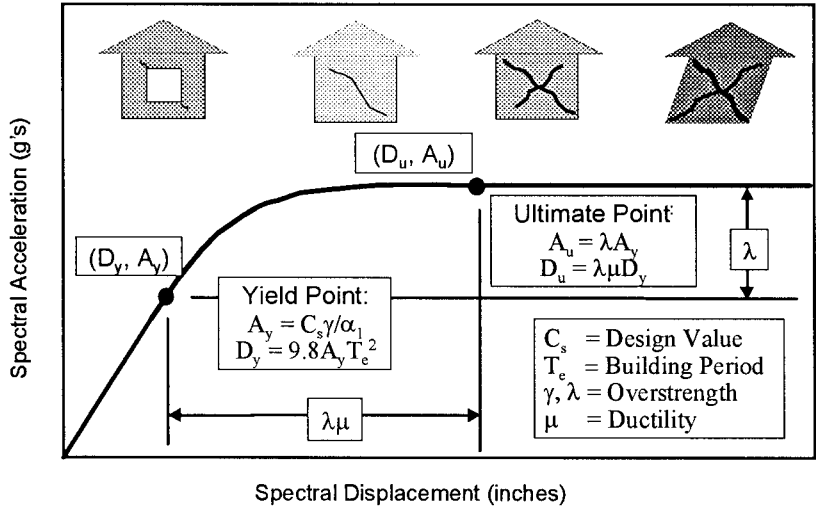

Figure 2. Example building capacity curve and control points

The following parameters define the yield point and the ultimate point of capacity curves as shown in Figure 2:

C_s design strength coefficient (fraction of building's weight),

T_e expected "elastic" fundamental-mode period of building (seconds),

α_1 fraction of building weight effective in the pushover mode,

α_2 fraction of building height at the elevation where pushover-mode displacement is equal to spectral displacement (not shown in Figure 2),

γ "overstrength" factor relating "true" yield strength to design strength,

λ "overstrength" factor relating ultimate strength to yield strength, and

μ "ductility" ratio relating ultimate displacement to λ times the yield displacement (i.e., assumed point of significant yielding of the structure)

The design strength, C_s, approximately corresponds to the lateral-force design requirements of current seismic codes (e.g., 1994 *UBC or* 1994 *NEHRP Provisions*) and is a function of the building's seismic zone location and other factors including site soil condition, type of lateral-force-resisting system and building period. Example design strength values are given in Table 3 for selected building types.

Table 3. Example building capacity parameters - design strength $(C_s)^1$

Building Type	Seismic Design Level			
	High-Code	Moderate-Code	Low-Code	Pre-Code
W1	0.200	0.150	0.100	0.100
S1L	0.133	0.067	0.033	0.033
S1M	0.100	0.050	0.025	0.025
S1H	0.067	0.033	0.017	0.017
C2L	0.200	0.100	0.050	0.050
URML	N/A	N/A	0.067	0.067

1. Shaded boxes indicate that URM buildings are not permitted by current seismic codes in zones corresponding to High-Code and Moderate-Code design levels.

The expected fundamental-mode period of the building, T_e, is calculated using the period formula of the *1994 UBC*, modified to reflect true building properties, and a height typical of the model building type (Table 1). Since the period specified by seismic codes is purposely set short to effect a conservative estimate of design force, the expected period of the building will typically be longer. Expected building periods are also used to account for flexing of diaphragms of short, stiff buildings, cracking of elements of concrete and masonry structures, flexibility of foundations, and other factors known to affect building stiffness.

For each Code design level (i.e., High-Code, Moderate-Code, Low-Code), building capacity is based on the best estimate of typical design properties (or effective design properties for Pre-Code buildings). Example values of expected building period, T_e, pushover mode parameters α_1 and α_2, the ratio of yield to design strength, γ, and the ratio of ultimate to yield strength, λ, are summarized in Table 4. Example values of the "ductility" factor, μ, are given in Table 5 for different code design levels.

Table 4. Example building capacity parameters - period (T_e), pushover modal response factors (α_1, α_2) and overstrength ratios (γ, λ)

Building Type	Height to Roof (ft)	Period, T_e (Seconds)	Modal Factors		Overstrength Ratios	
			Weight, α_1	Height, α_2	Yield, γ	Ultimate, λ
W1	14	0.35	0.75	0.75	1.50	3.00
S1L	24	0.50	0.75	0.75	1.50	2.50
S1M	60	1.08	0.75	0.75	1.25	2.00
S1H	156	2.21	0.65	0.60	1.10	2.00
C2L	20	0.35	0.75	0.75	1.50	2.50
URML	15	0.35	0.50	0.75	1.50	2.00

Table 5. Example building capacity parameters – ductility ratio (μ)

Building Type	Seismic Design Level			
	High-Code	Moderate-Code	Low-Code	Pre-Code
W1	8.0	6.0	6.0	6.0
S1L	8.0	6.0	5.0	5.0
S1M	5.3	4.0	3.3	3.3
S1H	4.0	3.0	2.5	2.5
C2L	8.0	6.0	5.0	5.0
URML	N/A	N/A	3.3	3.3

BUILDING RESPONSE

Building response is determined by the intersection of the demand spectrum and the building capacity curve. Intersections are illustrated in Figure 3 for three example demand spectra representing what can be considered as weak, medium and strong ground shaking, and two building capacity curves representing weaker and stronger construction, respectively. As shown in Figure 3, stronger and stiffer construction displaces less than weaker and more flexible construction for the same level of spectral demand, and less damage is expected to the structural system and nonstructural components sensitive to drift. In contrast, stronger construction will shake at higher acceleration levels, and more damage is expected to nonstructural components and contents sensitive to acceleration.

The demand spectrum is based on the 5%-damped response spectrum at the building's site (or centroid of a study area containing a group of buildings), reduced for effective damping when effective damping exceeds the 5% damping level of the input spectrum. Background on the 5%-damped response spectrum of ground shaking is provided in the next section.
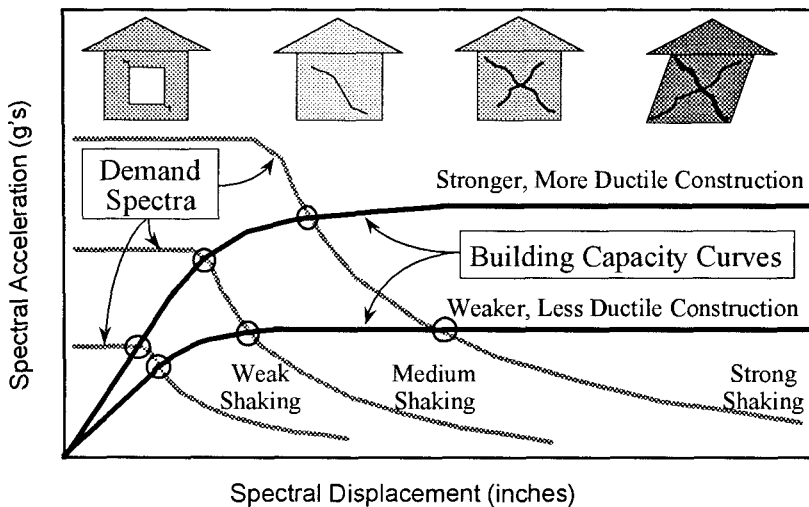

Figure 3. Example intersection of demand spectra and building capacity curves

GROUND SHAKING INPUT SPECTRUM

The FEMA/NIBS methodology characterizes ground shaking using a standard response spectrum shape, as shown in Figure 4, for spectra representing rock, stiff soil and soft soil conditions, respectively. The standard shape consists of two primary parts: (1) a region of constant spectral acceleration at short periods and (2) a region of constant spectral velocity at long periods. Short-period spectral acceleration, S_S, is defined by 5%-damped spectral acceleration at a period of 0.3 seconds. The constant spectral velocity region has spectral acceleration proportional to $1/T$ and is anchored to the 1-second, 5%-damped spectral acceleration, S_1. A region of constant spectral displacement exists at very long periods, although this region does not usually affect calculation of building damage and is not shown in Figure 4.
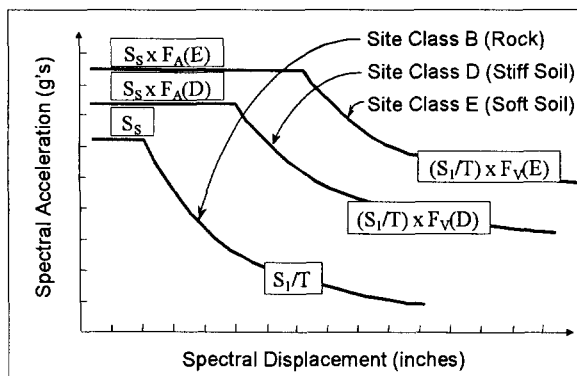

Figure 4. Example 5%-damped response spectra for three site classes

The FEMA/NIBS methodology predicts spectral response as a function of distance from scenario earthquake sources based on the same attenuation functions as those used by the United States Geological Survey to create national seismic hazard maps for *Project 97* (Frankel et al., 1996). These functions define ground shaking for rock (Site Class B) conditions based on earthquake magnitude and other source parameters (e.g., fault type).

Amplification of ground shaking to account for local site conditions is based on the soil factors of the *NEHRP Provisions*. The *NEHRP Provisions* define a standardized site geology classification scheme and specify soil amplification factors (i.e., F_A for the acceleration domain and F_V for the velocity domain). Figure 4 shows construction of demand spectra for stiff soil sites (Site Class D) and soft soil sites (Site Class E). These spectra illustrate the importance of soil type on spectral demand (and building response), particularly in the velocity domain.

DEMAND SPECTRUM - DAMPING REDUCTION

Extensive work has been published in the last two decades on modeling inelastic response of buildings. This work includes both explicit consideration of structural-system ductility (e.g., Miranda, 1993, Nassar, Osteraas and Krawinkler, 1992, Uang, 1991) and modification of elastic system properties (e.g., Kircher, 1996, Mahaney et al., 1993, Iwan and Gates, 1979). A recent study by Tsopelas et al. (1997) concludes that both approaches predict similar displacements for most buildings at ground shaking levels of design interest.

The FEMA/NIBS methodology is based on the latter modification of elastic system properties that simulates inelastic response by use of "effective" stiffness and damping properties of the building. Effective stiffness properties are based on secant stiffness, and effective damping is based on combined viscous and hysteretic measures of dissipated energy. Effective damping greater than 5% of critical is used to reduce spectral demand in a manner similar to the capacity-spectrum method of ATC-40 (SSC, 1996).

Figure 5 illustrates the process of developing an inelastic response (demand) spectrum from the 5%-damped elastic response (input) spectrum. The demand spectrum is based on elastic response divided by amplitude-dependent damping reduction factors (i.e., R_A at periods of constant acceleration and R_V at periods of constant velocity). The demand spectrum intersects the building's capacity curve at the point of peak response displacement, D, and acceleration, A. The amount of spectrum reduction typically increases for buildings that have reached yield and dissipate hysteretic energy during cyclic response.
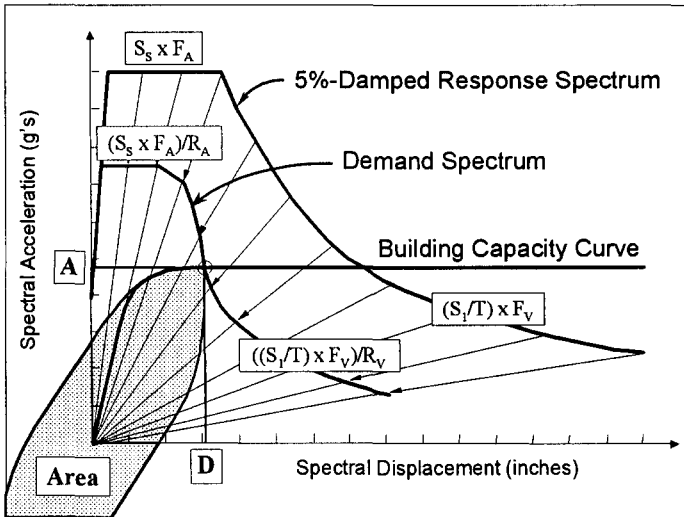

Figure 5. Example demand spectrum construction

Spectrum reduction factors are a function of the effective damping of the building, β_{eff}, as defined by Equations (1) and (2):

$$R_A = 2.12/(3.21 - 0.68\ln(\beta_{eff})) \qquad (1)$$

$$R_V = 1.65/(2.31 - 0.41\ln(\beta_{eff})) \qquad (2)$$

These equations are based on the formulas given in Table 2 of Newmark and Hall (1982) for construction of elastic response spectra at different damping levels (expressed as a percentage of critical damping). The factors of Newmark and Hall represent all site classes (soil profile types), but distinguish between domains of constant acceleration and constant velocity. For either domain, the reduction factor is the ratio of 5%-damped response to response of the system with β_{eff} damping. Equations (1) and (2) yield reduction values of R_A = 1.0 and R_V = 1.0, respectively, for a value of β_{eff} = 5% of critical.

Effective damping, β_{eff}, is defined as the total energy dissipated by the building during peak earthquake response and is the sum of an elastic damping term, β_E, and a hysteretic damping term, β_H, associated with post-yield, inelastic response:

$$\beta_{eff} = \beta_E + \beta_H \qquad (3)$$

The elastic damping term, β_E, is assumed to be a constant (i.e., amplitude independent) and follows the recommendations of Table 3 of Newmark & Hall for materials at or just below their yield points. Example values of the elastic damping term are given in Table 6.

The hysteretic damping term, β_H, is dependent on the amplitude of post-yield response and is based on the area enclosed by the hysteresis loop at peak response displacement, D, and acceleration, A, as shown in Figure 5. Hysteretic damping, β_H, is defined in Equation (4):

$$\beta_H = \kappa \left(\frac{\text{Area}}{2\pi\, D\, A} \right) \qquad (4)$$

where: Area   is the area enclosed by the hysteresis loop, as defined by a symmetrical push-pull of the building capacity curve up to peak positive and negative displacements, $\pm D$

D   is the peak displacement response of the capacity curve,

A   is the peak acceleration response at peak displacement, D

κ is a degradation factor that defines the fraction of the Area used to determine hysteretic damping (see Table 6 examples).

For a value of $\kappa = 1.0$, Equation (4) may be recognized as the definition of equivalent viscous damping, found in modern vibration textbooks (e.g., Chopra, 1995) and traceable to the early work by Jacobsen (1930) and others. The κ factor in Equation (4) reduces the amount of hysteretic damping as a function of model building type, seismic design level and shaking duration to simulate degradation (e.g., pinching) of the hysteresis loop during cyclic response. Shaking duration is described qualitatively as either short, moderate or long, and is assumed to be primarily a function of earthquake magnitude, although proximity to fault rupture can also influence the duration of the level of shaking that is most important to building damage. Example values of the degradation factor, κ, are given in Table 6.

Table 6. Example values of elastic damping and degradation factors (κ)

Building Type	Elastic Damping (β_E)	High-Code Design			Low-Code Design			Pre-Code Design		
		Duration of Strong Ground Shaking (Short, Moderate or Long)								
		Short	Mod.	Long	Short	Mod.	Long	Short	Mod.	Long
W1	15%	1.0	0.8	0.5	0.7	0.4	0.2	0.5	0.3	0.1
S1L	5%	0.9	0.6	0.4	0.6	0.3	0.1	0.4	0.2	0.0
S2L	7%	0.7	0.5	0.3	0.5	0.3	0.1	0.4	0.2	0.0
C2L	7%	0.9	0.6	0.4	0.6	0.3	0.1	0.4	0.2	0.0
URML	10%	N/A	N/A	N/A	0.5	0.3	0.1	0.4	0.2	0.0

Figure 6 shows a typical capacity curve and three example demand spectra for damping levels corresponding to short ($\kappa = 0.9$), moderate ($\kappa = 0.6$) and long ($\kappa = 0.4$) duration ground shaking, respectively. In this example, building displacement due to long-duration ground shaking is more than twice that due to short-duration ground shaking (although building acceleration does not increase). Damage to the structural system and nonstructural, drift-sensitive components and related losses increase significantly with increase in the duration of ground shaking for buildings that have reached yield.
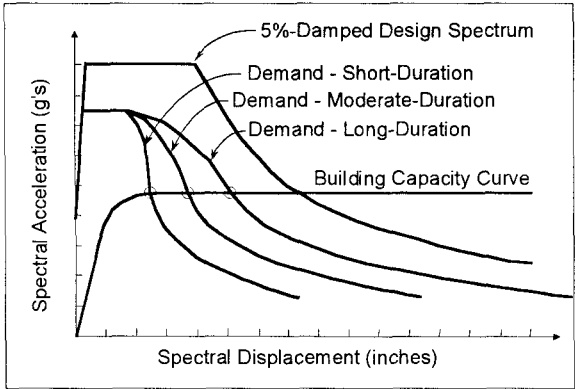

Figure 6. Example demand spectra – strong ground shaking of short, moderate and long-duration

BUILDING FRAGILITY CURVES

Building fragility curves are lognormal functions that describe the probability of reaching, or exceeding, structural and nonstructural damage states, given deterministic (median) estimates of spectral response, for example spectral displacement. These curves take into account the variability and uncertainty associated with capacity curve properties, damage states and ground shaking.
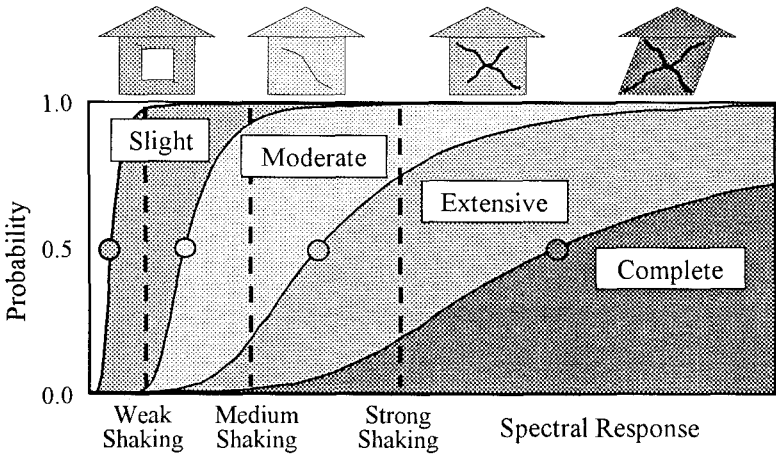

Figure 7. Example fragility curves for Slight, Moderate, Extensive and Complete damage

Figure 7 provides an example of fragility curves for the four damage states used in the FEMA/NIBS methodology and illustrates differences in damage-state probabilities for three levels of spectral response corresponding to weak, medium, and strong earthquake ground shaking, respectively. The terms "weak," "medium," and "strong" are used here for simplicity; in the actual methodology, only quantitative values of spectral response are used.

The fragility curves distribute damage among Slight, Moderate, Extensive and Complete damage states. For any given value of spectral response, discrete damage-state probabilities are calculated as the difference of the cumulative probabilities of reaching, or exceeding successive damage states. Discrete damage-state probabilities are used as inputs to the calculation of various types of building-related loss. Figure 8 provides an example of discrete damage state probabilities for the three levels of earthquake ground shaking.
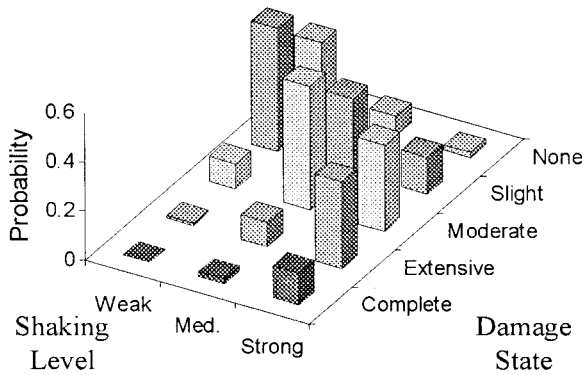

Figure 8. Example damage-state probabilities for weak, medium and strong shaking levels

Each fragility curve is defined by a median value of the demand parameter (e.g., spectral displacement) that corresponds to the threshold of that damage state and by the variability associated with that damage state. For example, the spectral displacement, S_d, that defines the threshold of a particular damage state (ds) is given by Equation (5):

$$S_d = \overline{S}_{d,ds} \ \varepsilon_{ds} \tag{5}$$

where: $\overline{S}_{d,ds}$ is the median value of spectral displacement of damage state, ds,

ε_{ds} is a lognormal random variable with a unit median value and a logarithmic standard deviation, β_{ds}.

In a more general formulation of fragility curves, the lognormal standard deviation, β, has been expressed in terms of the randomness and uncertainty components of variability, β_R and β_U, respectively [Kennedy, et. al., 1980]. In the Kennedy formulation, uncertainty represents the component of the variability that could theoretically be reduced with improved knowledge, whereas randomness represents the inherent variability (in response) that cannot be eliminated, even with perfect knowledge. Since it is not considered practical to separate uncertainty from randomness, the combined variability, β, is used to develop a composite "best-estimate"

fragility curve. This approach is similar to that used to develop fragility curves for the FEMA-sponsored study of consequences of a large earthquake on six cities of the Mississippi Valley region (Kircher and McCann, 1983).

The conditional probability of being in, or exceeding, a particular damage state, ds, given the spectral displacement, S_d, (or other seismic demand parameter) is defined by Equation (6):

$$P[ds| S_d] = \Phi\left[\frac{1}{\beta_{ds}} \ln\left(\frac{S_d}{\overline{S}_{d,ds}}\right)\right] \tag{6}$$

where: $\overline{S}_{d,ds}$ is the median value of spectral displacement at which the building reaches the threshold of damage state, ds,

β_{ds} is the standard deviation of the natural logarithm of spectral displacement for damage state, ds, and

Φ is the standard normal cumulative distribution function.

DAMAGE-STATE MEDIANS

Median values of fragility curves are developed for each damage state (i.e., Slight, Moderate, Extensive and Complete) of each of the three types of building systems: structural, nonstructural drift-sensitive components and nonstructural acceleration-sensitive components. In general, median fragility values are also different for each seismic design and performance level.

Structural fragility is expressed in terms of spectral displacement, except for lifeline buildings whose fragility functions are expressed in terms of peak ground acceleration for compatibility with lifeline equipment fragility. Median values of structural component fragility are based on inter-story drift ratios that describe the threshold of damage states. Damage-state drift ratios are converted to spectral displacement using Equation (7):

$$\overline{S}_{d,ds} = \delta_{ds}\, \alpha_2\, H \tag{7}$$

where: $\overline{S}_{d,ds}$ is the median value of spectral displacement for damage state, ds,

δ_{ds} is the drift ratio at the threshold of structural damage state, ds,

α_2 is the fraction of the building (roof) height at the elevation where pushover-mode displacement equals spectral displacement, and

H   is the typical roof height of the model building type of interest.

Values of damage-state drift ratios included in the FEMA/NIBS methodology are based, in part, on available damage data from a number of published sources, including Kustu et al. (1982), Ferritto (1982 and 1983), Czarnecki (1973), Hasselman et al. (1980), Whitman et al. (1977) and Wong (1975). Drift ratios are different for each model building type (including height-defined sub-types) and seismic design level. Table 7 summarizes typical drift ratios used to define structural damage for various building types. In Table 7, drift ratios decrease with building height to account for anticipated non-uniform distribution of drift over the height of the building (i.e., the taller the building, the more likely some floors will have higher than average drifts).

Table 7. Typical drift ratios used to define structural damage states

Design Level	Model Building Type	Drift Ratio at the Threshold of Structural Damage			
		Slight	Moderate	Extensive	Complete
High-Code	W1	0.004	0.012	0.040	0.100
	S1L	0.006	0.012	0.030	0.080
	S1M	0.004	0.008	0.020	0.053
	S1H	0.003	0.006	0.015	0.040
	C2L	0.004	0.010	0.030	0.080
Moderate-Code	W1	0.004	0.010	0.031	0.075
	S1L	0.006	0.010	0.024	0.060
	C2L	0.004	0.008	0.023	0.060
Low-Code	W1	0.004	0.010	0.031	0.075
	S1L	0.006	0.010	0.020	0.050
	C2L	0.004	0.008	0.020	0.050
	URML	0.003	0.006	0.015	0.035
Pre-Code	W1	0.003	0.008	0.025	0.060
	S1L	0.005	0.008	0.016	0.040
	C2L	0.003	0.006	0.016	0.040
	URML	0.002	0.005	0.012	0.028

Nonstructural drift-sensitive component fragility is based on spectral displacement, as is structural system fragility. As in Equation (7), median values of spectral displacement are expressed in terms of the product of (1) damage-state drift ratios, (2) the fraction of building height at the elevation where pushover mode equals spectral displacement (α_2), and (3) typical roof height of the model building type.

Damage-state drift ratios are based, in part, on the work of Ferritto (1982 and 1983) and on a recent update of this data included in a California Division of the State Architect report (DSA, 1996). Table 8 summarizes the drift ratios used to develop median values of fragility curves for drift-sensitive nonstructural components of buildings. Nonstructural damage drift ratios are assumed independent of model building type and seismic design level.

Table 8. Drift ratios used to define median values of fragility curves for nonstructural drift-sensitive components

Drift Ratio at the Threshold of Nonstructural Damage			
Slight	Moderate	Extensive	Complete
0.004	0.008	0.025	0.050

Nonstructural acceleration-sensitive component fragility is based on peak floor acceleration, taken as either peak ground acceleration for evaluation of components located at or near the base of the building, or average upper-floor peak acceleration for evaluation of components located in the upper stories of the building. Average upper-floor acceleration is assumed to be equal to the spectral acceleration defined by the capacity curve.

Median values of damage-state spectral acceleration are based, in part, on the work of Ferritto (1982 and 1983) and on a recent update of this data included in a DSA report (1996). Table 9 summarizes the peak floor accelerations used to define median values of fragility curves for acceleration-sensitive nonstructural components of buildings. Nonstructural damage acceleration values are the same for each model building type, but vary by seismic design level to account for different levels of seismic restraint and/or anchorage.

Table 9. Peak floor accelerations used to define median values of fragility curves for nonstructural acceleration-sensitive components

Seismic Design Level	Peak Floor Acceleration at the Threshold of Nonstructural Damage (g)			
	Slight	Moderate	Extensive	Complete
High-Code	0.30	0.60	1.20	2.40
Moderate-Code	0.25	0.50	1.00	2.00
Low-Code	0.20	0.40	0.80	1.60
Pre-Code	0.20	0.40	0.80	1.60

DAMAGE-STATE VARIABILITY

Lognormal standard deviation values (β) describe the total variability of fragility-curve damage states. Three primary sources contribute to the total variability of any given state, namely, the variability associated with the capacity curve, β_C, the variability associated with the demand spectrum, β_D, and the variability associated with the discrete threshold of each damage state, $\beta_{T,ds}$, as described in Equation (8):

$$\beta_{ds} = \sqrt{(\text{CONV}[\beta_C, \beta_D])^2 + (\beta_{T,ds})^2} \qquad (8)$$

where: β_{ds} is the lognormal standard deviation parameter that describes the total variability of damage state, ds,

β_C is the lognormal standard deviation parameter that describes the variability of the capacity curve,

β_D is the lognormal standard deviation parameter that describes the variability of the demand spectrum,

$\beta_{T,ds}$ is the lognormal standard deviation parameter that describes the variability of the threshold of damage state, ds.

Since the demand spectrum is dependent on building capacity, a convolution process is required to combine their respective contributions to total variability. This is referred to as "CONV" in Equation (8) and is described below. The third contributor to total variability, $\beta_{T,ds}$, is assumed mutually independent of the first two variables and is combined with the results of the CONV process using the square-root-sum-of-the squares (SRSS) method.

The convolution process is graphically illustrated by a three-dimensional (3D) surface as shown in Figure 11. This surface defines the joint probability function of intersection points of capacity and demand in the spectral displacement-spectral acceleration (S_d-S_a) domain. For any given building type, a unique median capacity curve is defined as described in the previous

section. A suite of curves representing other (non-median) probability levels characterizes capacity variability in the S_d-S_a domain. Each of these curves has a probability defined by the lognormal standard deviation parameter, β_C, and a shape that maintains the relationship between yield and ultimate points, as shown in Figure 2. In 3D space, the distribution of possible capacity curves looks like a bell curve moving along the median.
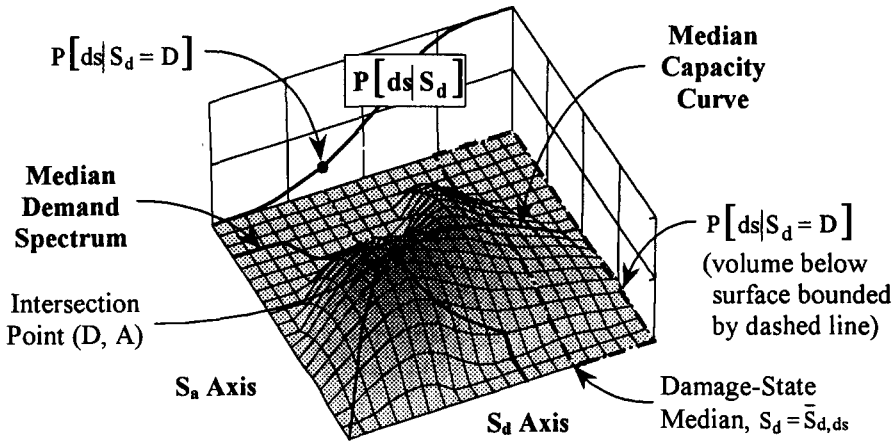

Figure 11. Example joint probability surface of demand and capacity intersection points. *In color:* see plates following p. 738.

The median demand spectrum is defined by a generic shape scaled to represent different levels of ground shaking (i.e., different distances from the source). In general, the shape of the median demand spectrum is a function of a number of factors, including source magnitude and type, and site conditions. For the purpose of defining demand variability, the shape of the median demand spectrum is assumed to be the same for all source and site conditions. A suite of demand curves representing other (non-median) probability levels characterizes demand variability in the S_d-S_a domain. Each of these curves has a probability defined by the lognormal standard deviation parameter, β_D, and the same shape as median spectral demand.

The joint probability surface shown in Figure 11 is the cross-product of demand and capacity probability functions, discretely characterized by the suites of demand and capacity curves described above. The shape of surface is an indicator of response variability; the greater the variability of capacity and demand, the flatter the surface. On the other hand, if capacity and demand were known exactly (which is not realistic), the surface would converge to a spike at the intersection point of median demand and capacity (D, A).

Vertical planes in 3D space are used to calculate damage distributions for each of the three building systems: structural, nonstructural drift-sensitive and nonstructural acceleration-sensitive components. Planes normal to the S_d axis represent the first two systems, while planes normal to the S_a axis represent the latter system. Each plane is defined by the median value of the damage state. There are 12 vertical planes in total, representing four damage states for each of the three building systems.

The volume under the entire 3D surface shown in Figure 11 is 100%, representing all possible intersections of demand and capacity in the S_d-S_a domain. The probability of reaching

or exceeding a given damage state, ds, for a given building system is the volume under the 3D surface for values of S_d (or S_a) greater than median value of S_d (or S_a) that defines the plane representing the damage state. For example, a dashed line in Figure 11 bounds the portion of the 3D surface used to calculate the probability of damage state, ds, given spectral displacement, $S_d = D$.

Each 3D surface represents a specific level of seismic demand and yields one probability value for each of the 12 damage distributions. For example, Figure 11 shows the probability of damage state, ds, for this surface, $P[ds|S_d = D]$, as a point on the cumulative distribution, $P[ds|S_d]$. A number of 3D surfaces are constructed at different seismic demand levels to fully define each of the 12 damage distributions. Visually, the intersection point (D, A) moves in the S_d-S_a domain as the seismic demand level changes, but the 12 damage-state planes remain fixed in space. The damage distribution, $P[ds|S_d]$, shown in Figure 11, is calculated by fitting a lognormal distribution to discrete values of cumulative probability.

In general, the variability of capacity, demand and damage-state thresholds all contribute significantly to the total variability of structural and nonstructural damage states. Lognormal standard deviation values of total damage-state variability are generally in the range of $\beta_{ds} = 0.65$ to 1.2. Although large, these estimates of total variability are reasonable considering that the variability of spectral demand alone is about $\beta_D = 0.5$. Large values of damage-state variability suggest that improved knowledge of building capacity curves and damage-state thresholds could appreciably reduce uncertainty in damage estimates. However, damage-state variability can never be less than the variability of spectral demand, and damage estimates will always have uncertainty due to the inherent variability of earthquake ground shaking.

Reducing damage-state variability would have a limited effect on the probability of damage for demand levels at or near the median value of the damage state of interest. On the other hand, reducing variability would significantly change the probability of damage for demand levels that are much smaller than the median of the given damage state. The latter condition is typical of estimates of Extensive or Complete damage, which tend to have small probabilities (i.e., less than 0.10) even for strong ground shaking. Improved knowledge of building capacity and damage states would be most useful for better estimation of the probabilities of Extensive or Complete damage, and those losses, such as fatalities or loss of function, that are most dependent on these states of damage. In contrast, economic loss is less sensitive to damage-state variability, since all damage states contribute significantly to this type of loss.

CONCLUSION

This paper has described building damage functions of the FEMA/NIBS earthquake loss estimation methodology. These functions estimate probabilities of building damage states based on quantitative measures of ground shaking (response spectra). Damage-state probabilities are used by the FEMA/NIBS methodology as inputs to the estimation of building losses, including economic loss, casualties and loss of function.

Building damage functions are of a new form and represent a significant step forward in the prediction of earthquake impacts. These functions now permit loss estimation to incorporate important ground shaking characteristics, including site/soil amplification effects and shaking duration. Further, these functions explicitly consider the differences among
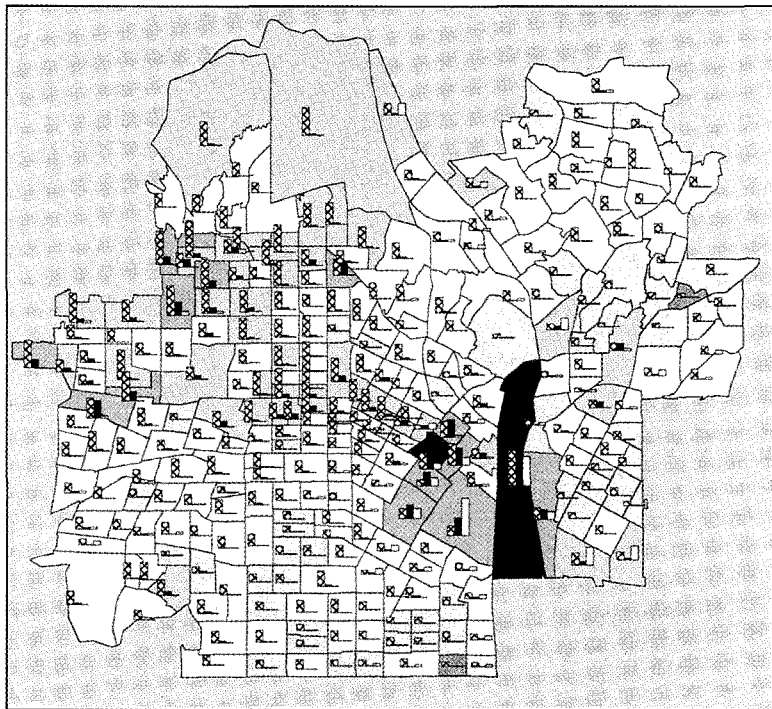
6) Thematic map of total economic losses for a scenario event. From Whitman et al., p. 655.
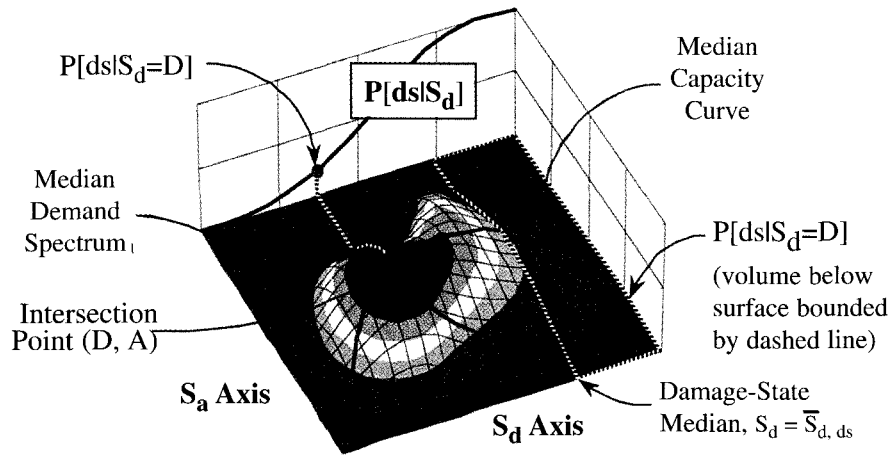
7) Example joint probability surface of demand and capacity intersection points. From Kircher et al., p. 680.

buildings based on their seismic design level and vintage, and anticipated performance, explicitly considering nonlinear inelastic response, and its effects on the structural system, nonstructural components, and contents of the building.

FEMA/NIBS building damage functions provide rational tools for quantitative evaluation of building losses and mitigation alternatives that previously could only be judged in a qualitative manner. With these tools, engineers and planners can begin to develop strategies for earthquake hazard mitigation that combine both elements of pre-event action and post-event response and recovery using more reliable engineering data.

REFERENCES

Chopra, Anil K., 1995. *Dynamics of Structures*. (Engelwood Cliffs, New Jersey: Prentice Hall).

Czarnecki, Robert M., 1973. *Earthquake Damage to Tall Buildings*. (Cambridge, MA: Structures Publication No. 359. Department of Civil Engineering, Massachusetts Institute of Technology).

Division of the State Architect (DSA), 1996. *Earthquake Hazard Mitigation Technology, Application Guidelines and Recommendations*. (Sacramento, CA: California Department of General Services).

Earthquake Engineering Research Institute (EERI), 1994. *Expected Seismic Performance of Buildings*. (Oakland, CA: EERI).

Federal Emergency Management Agency (FEMA), 1997. *NEHRP Guidelines for the Seismic Rehabilitation of Buildings*, Ballot Version. (Washington, D.C.: FEMA 273).

Federal Emergency Management Agency (FEMA), 1995. *NEHRP Recommended Provisions for the Seismic Regulations for New Buildings*. (Washington, D.C.: FEMA 222A).

Federal Emergency Management Agency (FEMA), 1992. *NEHRP Handbook for the Seismic Evaluation of Existing Buildings*. (Washington, D.C.: FEMA 178).

Ferritto, J.M., 1982. *An Economic Analysis of Earthquake Design Levels*. (Port Hueneme, CA: Department of the Navy Civil Engineering Laboratory, TN No. N-1640).

Ferritto, J.M., 1983. *An Economic Analysis of Earthquake Design Levels for New Concrete Construction*. (Port Hueneme, CA: Department of the Navy Civil Engineering Laboratory., TN No. N-1671).

Frankel, Arthur, Charles Mueller, Theodore Barnhard, David Perkins, E.V. Leyendecker, Nancy Dickman, Stanley Hanson and Margaret Hopper, 1997. "National Seismic-Hazard Maps," United States Geological Survey (USGS) Open-File Reports 96-532 and 96-706. (Denver, CO: USGS).

Hasselman, T.K., Ronald T. Eguchi, and John H. Wiggins, 1980. *Assessment of Damageability for Existing Buildings in a Natural Hazards Environment. Volume I: Methodology*. (Redondo Beach, CA).

International Conference of Building Officials (ICBO), 1994. *Uniform Building Code* (Whittier, CA: ICBO).

Iwan, W.D. and Gates, N.C., 1979, "Estimating Earthquake Response of Simple Hysteretic Structures," *Journal of Engineering Mechanics Division*, 105(EM3), pp. 391-405. (Washington, D.C.: American Society of Civil Engineers).

Kennedy, R.P., C.A. Cornell, R.L. Campbell, S. Kaplan and H.F. Perla, 1980. "Probabilistic Seismic Safety of an Existing Nuclear Power Plant," *Nuclear Engineering and Design*, Vol. 59(2): pp. 315-38.

Kircher, Charles A., Robert K. Reitherman, Robert V. Whitman and Christopher Arnold, 1997. "Estimation of Earthquake Losses to Buildings, " *Earthquake Spectra*, Vol. 13, No. 4, (Oakland, CA: Earthquake Engineering Research Institute).

Kircher, Charles A., 1996. "Capacity Spectrum Pushover Method: Seeing is Believing," Proceedings 65th Annual Convention. (Sacramento, CA: Structural Engineers Association of California).

Kircher, Charles A. and Martin W. McCann, 1983. "Development of Fragility Curves for Estimation of Earthquake-Induced Damage." *Workshop on Continuing Actions to Reduce Losses from Earthquakes in Arkansas and Nearby States.* (Washington, DC: United States Geological Survey).

Kustu, O., D. D. Miller, and S. T. Brokken, 1982. *Development of Damage Functions for High-Rise Building Components.* (San Francisco, CA: URS/John A. Blume & Associates report prepared for U.S. Department of Energy).

Jabobsen, L. S., 1930. "Steady Forced Vibration as Influenced by Damping," Trans. ASME, APM-52-15, 1930. (New York, New York: American Society of Mechanical Engineers).

Mahaney, J. A., T. F. Paret, B. E. Kehoe and S. A. Freeman, 1993. "The Capacity Spectrum Method for Evaluating Structural Response During the Loma Prieta Earthquake," *1993 U.S. Earthquake Conference,* (Oakland, CA: Earthquake Engineering Research Institute).

Miranda, E., 1993. "Evaluation of Site-Dependent Inelastic Seismic Design Spectra," *Journal of the Structural Engineering Division,* Vol. 119, No. 5, pp. 1319-1338. (New York, NY: American Society of Civil Engineers).

Nassar, Aladdin A., John D. Osteraas, Helmut Krawinkler, 1992. "Seismic Design based on Strength and Ductility," *Proceedings of the 10th World Conference on Earthquake Engineering (10WCEE),* July 19-24, 1992, Madrid, Spain, Vol. 10, pp. 5861-5866.

National Institute of Building Science (NIBS), 1997. *Earthquake Loss Estimation Methodology, HAZUS97: Technical Manual.* Report prepared for the Federal Emergency Management Agency. (Washington, D.C.: NIBS).

Newmark, N. M. and W. J. Hall, 1982. *Earthquake Spectra and Design.* Earthquake Engineering Research Institute (EERI) Monograph. (Oakland, CA: EERI).

Seismic Safety Commission (SSC), 1996. *Seismic Evaluation and Retrofit of Concrete Buildings,* SSC Report No. 96-01 (Sacramento, CA: Seismic Safety Commission, State of California).

Steinbrugge, Karl V., 1982. *Earthquake, Volcanoes, and Tsunamis: An Anatomy of Hazards.* (New York: Skandia America Group).

Tsopelas, P., M. C. Constantinou, C. A. Kircher and A. S. Whittaker, 1997. "Evaluation of Simplified Methods of Analysis for Yielding Structures," National Center for Earthquake Engineering Research Technical Report NCEER-97-0012 (Buffalo, NY: State University of New York).

Uang, Chia-M., 1991. "Establishing R (or R_w) and C_d Factors for Building Seismic Provisions." *Journal of the Structural Engineering Division, Vol. 117, No.1: pp. 19-28.* (New York, NY: American Society of Civil Engineers).

Whitman, Robert V., Thalia Anagnos, Charles A. Kircher, Henry J. Lagorio, R. Scott Lawson, Philip Schneider, 1997. "Development of a National Earthquake Loss Estimation Methodology," *Earthquake Spectra,* Vol. 13, No. 4, (Oakland, CA: Earthquake Engineering Research Institute).

Whitman, Robert V., Tarek S. Aziz and Earl H. Wong, 1977. *Preliminary Correlations Between Earthquake Damage and Strong Ground Motion.* (Cambridge, MA: Structures Publication No. 564, Department of Civil Engineering, Massachusetts Institute of Technology).

Whitman, Robert V., et al., 1974. *Methodology and Pilot Application.* (Cambridge, MA: Department of Civil Engineering, Massachusetts Institute of Technology).

Whitman, Robert V., J. W. Reed, and S. T. Hong, 1973. "Earthquake Damage Probability Matrices," *Proceedings of the Fifth World Conference on Earthquake Engineering.*

Wong, Earl Hom, 1975. *Correlations Between Earthquake Damage and Strong Ground Motion.* (Cambridge, MA: Department of Civil Engineering, M.I.T.)